Polymers **2014**, *6*, 264-279; doi:10.3390/polym6020264

OPEN ACCESS

polymers

ISSN 2073-4360

www.mdpi.com/journal/polymers

Article

RGD-Functionalization of Poly(2-oxazoline)-Based Networks for Enhanced Adhesion to Cancer Cells

Verena Schenk [1,2], Elisabeth Rossegger [1,2], Clemens Ebner [1], Florian Bangerl [2], Klaus Reichmann [2], Björn Hoffmann [3], Michael Höpfner [3,*] and Frank Wiesbrock [1,*]

[1] Polymer Competence Center Leoben GmbH PCCL, Roseggerstrasse 12, Leoben 8700, Austria; E-Mails: verena.schenk@pccl.at (V.S.); elisabeth.rossegger@pccl.at (E.R.); clemens.ebner@pccl.at (C.E.)

[2] Institute for Chemistry and Technology of Materials, Graz University of Technology, Stremayrgasse 9, Graz 8010, Austria; E-Mails: bangerl@student.tugraz.at (F.B.); k.reichmann@tugraz.at (K.R.)

[3] Institute of Physiology, Charité, Universitätsmedizin Berlin, Campus Charité Mitte, Charitéplatz 1, Berlin 10117, Germany; E-Mail: bjoern.hoffmann@charite.de

* Authors to whom correspondence should be addressed; E-Mails: michael.hoepfner@charite.de (M.H.); frank.wiesbrock@pccl.at (F.W.); Tel.: +49-30-450-528515 (M.H.); +43-3842-42962-42 (F.W.); Fax: +49-30-450-528920 (M.H.); +43-3842-42962-6 (F.W.).

Received: 16 November 2013; in revised form: 8 January 2014 / Accepted: 15 January 2014 / Published: 27 January 2014

Abstract: Poly(2-oxazoline) networks with varying swelling degrees and varying hydrophilicity can be synthesized from 2-ethyl-2-oxazoline, 2-nonyl-2-oxazoline, 2-9'-decenyl-2-oxazoline and 2,2'-tetramethylene-bis-2-oxazoline in one-pot/one-step strategies. These gels can be loaded with organic molecules, such as fluorescein isothiocyanate, either during the polymerization (covalent attachment of the dye) or according to post-synthetic swelling/deswelling strategies (physical inclusion of the dye). Surface functionalization of ground gels by thiol-ene reactions with cysteine-bearing peptides exhibiting the arginine-glycine-aspartic acid (RGD) motif yields microparticles with enhanced recognition of human cancer cells compared to healthy endothelial cells.

Keywords: poly(2-oxazoline)s; crosslinked polymer networks; RGD interaction with integrins; cancer cell recognition

---

1. Introduction

Biocompatible and, in particular, biodegradable hydrogels [1–3] are in use in a broad range of medical and medicinal applications, such as tissue engineering [4] and drug delivery [5]. Drugs can be released from hydrogels by diffusion, degradation of the hydrogels or combined strategies [6]. Crosslinking of poly(2-oxazoline)s can be realized either *in situ* (during the copolymerizations themselves) or after the copolymerizations (so-called polymeranalogous strategies) [7]. Poly(2-oxazoline)-based hydrogels are interesting candidates for various biomedical applications [2,8]. Like other synthetic or natural polymers, poly(2-oxazoline)s have been functionalized with peptide structures in order to enhance cell adhesion, concomitant with increased biocompatibility and cell-specific drug delivery characteristics. However, reports on that specific topic are rather scarce [9]. The functionalization of polymers with peptide units of arginine-glycine-aspartic acid (RGD) has been under extensive research in recent years [10–14], and combinations of polymer-based materials with constrained pentacyclic peptides, like c(RGDfC) [15,16], have been reported [10,17]. The mechanism of RGD motif recognition and subsequent cell attachment is based on the presence of integrins on cell surfaces. In particular, the $\alpha_v\beta_5$-integrin and its $\alpha_v\beta_3$ congener have been reported to show strong interaction with the cyclic RGD motif [18,19]. Due to the known overexpression, as well as the high activity of integrins in tumor cells [20,21], research started to focus on the preparation of RGD-functionalized hydrogels for enhanced cancer imaging and for the development of targeted strategies for cancer treatment [9,22]. Nonetheless, the investigation of these phenomena is still in its infancy.

Microwave-assisted chemistry has been shown to accelerate the polymerizations of 2-oxazolines by the straightforward provision of autoclave conditions, and this subsequently promoted the investigation of poly(2-oxazoline)s [23–27]. Notably, a recent study of the regioselectivity during the initiation of the cationic ring-opening polymerization of 2-oxazolines has revealed that only the nitrogen atoms, but not the oxygen atoms, of the 2-oxazoline pentacycles can react with the initiating cations (Scheme 1) [28]. Hence, the cationic ring-opening polymerization yields polymers with highly predictable structures and narrow average molecular weight distributions [26], which are key prerequisites for subsequent biomedical use. Termination of the polymerization with, e.g., anions or reactants that can be deprotonated yields end-group functionalized poly(2-oxazoline)s [29].

Scheme 1. Mechanism of the cationic ring-opening polymerization (CROP) of 2-ethyl-2-oxzoline initiated by methyl tosylate (**MeOTs**) and terminated by fluorescein isothiocyanate (**FITC**).

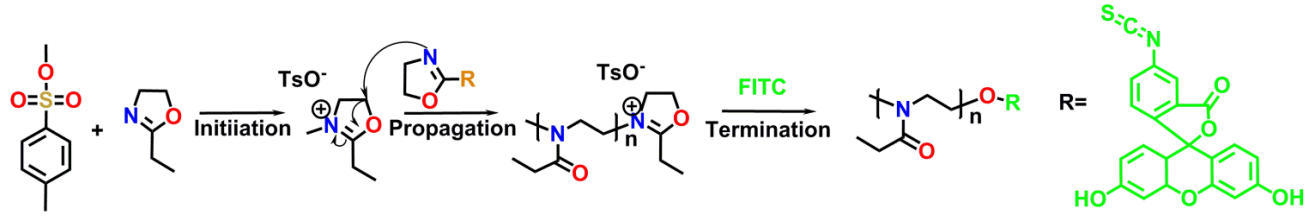

Preceded by the systematic investigation of poly(2-oxazoline) networks bearing aromatic side-chains [30], this study aimed for the synthesis of aromatic-free poly(2-oxazoline) gels with varying swelling degrees and hydrophilicity. Three monofunctional monomers, 2-ethyl-2-oxazoline

(**EtOx**), 2-nonyl-2-oxazoline (**NonOx**) and 2-9'-decenyl-2-oxazoline (**Dc$^{=}$Ox**) were crosslinked with aliphatic bis-2-oxazoline 2,2'-tetramethylene-bis-2-oxazoline (**TMBO**) (Scheme 2). The variation of the monomer composition aimed for the synthesis of lipo-, hydro- and amphi-gels. The gels were subsequently tested for loadability with the fluorescent dye, fluorescein isothiocyanate (**FITC**) (Scheme 1). Inclusion of **Dc$^{=}$Ox** with unsaturated side-chains in the copoly(2-oxazoline) chains enabled the surface functionalization of ground hydrogels by thiol-ene reactions [31–33]. Notably, due to *in situ* crosslinking with a bisfunctional monomer and subsequent functionalization by thiol-ene, the reactions enabled orthogonal syntheses. As thiol, cysteine-bearing peptides exhibiting the RGD motif in constrained geometries [cyclo(Arg-Gly-Asp-D-Phe-Cys) c(RGDfC)] were employed. The surface-functionalized gels were tested for enhanced binding to human cancer cells with a high expression of $\alpha_v\beta_5$- and $\alpha_v\beta_3$-integrins on the one hand, and to non-transformed endothelial cells, on the other.

Scheme 2. Copolymerization of 2-ethyl-2-oxazoline (**EtOx**), 2-nonyl-2-oxazoline (**NonOx**) and 2-9'-decenyl-2-oxazoline (**Dc$^{=}$Ox**) and aliphatic bis-2-oxazoline 2,2'-tetramethylene-bis-2-oxazoline (**TMBO**) for the synthesis of poly(2-oxazoline)-based gels (top) and subsequent (surface) functionalization with the cyclic pentapeptide c(RGDfC) by thiol-ene reactions (bottom).

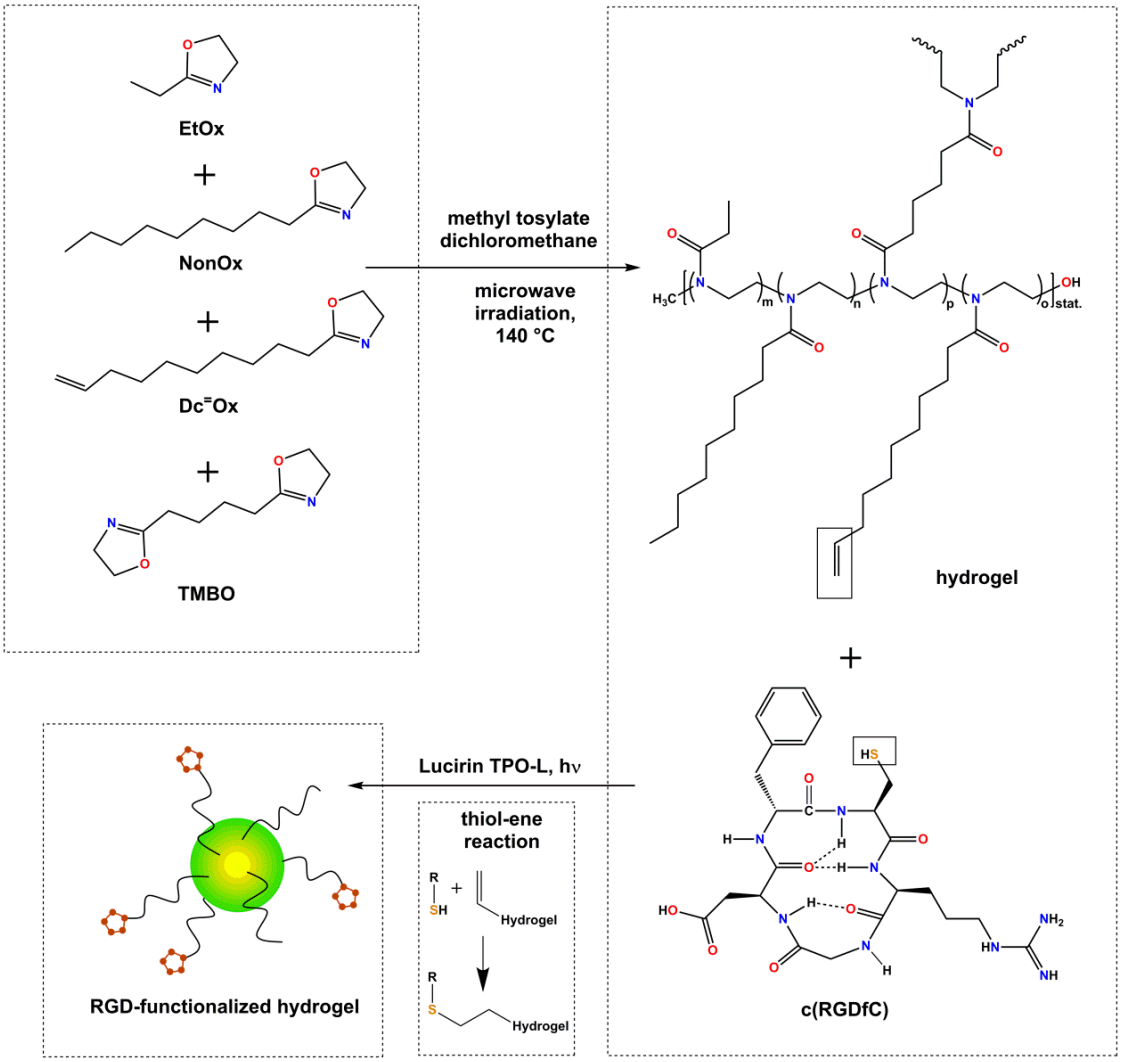

2. Experimental Section

Materials. All materials were purchased from Sigma-Aldrich (Vienna, Austria), unless indicated otherwise. c(RGDfC) was purchased from Bachem AG (Bubendorf, Switzerland). Lucirin TPO-L (2,4,6-trimethylbenzoylethylphenylphosphinate) was provided by Ciba (now BASF, Ludwigshafen, Germany). All chemicals were used as received, unless indicated otherwise. Commercially available **EtOx** and methyl tosylate (**MeOTs**) were distilled prior to use. **TMBO** was synthesized according to a literature recipe from adiponitrile and ethanol-2-amine [34] (catalyst: cadmium acetate dihydrate) with yields of 25 g (72%) after purification. **NonOx** was prepared according to a literature recipe from decanoic acid and ethanol-2-amine [35] [catalyst: titanium(IV) *n*-butoxide] with a yield of 80 g (71%) after purification. **Dc$^{=}$Ox** was analogously synthesized from undecenoic acid and ethanol-2-amine [catalyst titanium(IV) *n*-butoxide] with a yield of 60.0 g (58%) after purification. Deionized water was produced through reverse osmosis.

Instrumentation. Microwave-assisted hydrogel syntheses were performed in sealed vials in the single-mode microwave reactor, Biotage Initiator 8. All reactions were carried out in temperature-controlled modes; the reaction temperature was monitored by a non-invasive IR pyrometer. Removal of excess solvent during the determination of swelling degrees was performed in a Chromabond solid-phase extractor (Macherey Nagel, Dueren, Germany). The hydrogels were ground in a Retsch S1000 planetary ball mill as aqueous suspensions (100 mg/15 mL) for 24 h. Particle sizes were determined with a CILAS 1180 Particle Size Analyzer (CILAS, Orleans, France). Thiol-ene photoreactions were performed with Hg/Xe lamps of the EFOS Novacure (EFOS, Mississauga, Canada) from EXFO equipped with a light guide for the transfer of the UV light in close vicinity to the suspensions to be illuminated (8-cm distance). Transmission light and green fluorescence microscopy (ex/em ~495 nm/~510 nm) were monitored with a fluorescence microscope from Zeiss (Axioskop-2; Jena, Germany), digitalized with a Kappa DX-4 camera (Kappa, Gleichen, Germany) and stored and analyzed with Kappa camera control software (version 1.4.0.8053). Scanning electron microscopy energy dispersive X-ray (SEM-EDX) measurements were performed using a Tescan Vega 3 scanning electron microscope with an energy dispersive X-ray spectrometer (EDX Oxford Instruments INKAx-act, Abington, United Kingdom) attached. Electron energy levels were set to 20 kV.

Hydrogel Syntheses and Purifications. Hydrogels were synthesized under microwave irradiation from **EtOx**, **NonOx**, **Dc$^{=}$Ox** and **TMBO** with **MeOTs** as the initiator using anhydrous dichloromethane as the solvent. The ratios of monofunctional 2-oxazolines were chosen from [**EtOx**]:[**NonOx**]:[**Dc$^{=}$Ox**] = 150:0:0, 100:0:50, 50:50:50, 0:100:50, or 0:150:0 (5 variations); the ratio [**MeOTs**]:[sum of monofunctional 2-oxazolines] was constant at 1:150, and the ratio [sum of monofunctional 2-oxazolines]:[**TMBO**] was varied according to 150:30, 150:15, 150:10, 150:7.5 and 150:6 (5 combinations). In a typical procedure, a reaction mixture containing the components in a ratio of [**EtOx**]:[**NonOx**]:[**Dc$^{=}$Ox**]:[**TMBO**]:[**MeOTs**] = 100:0:50:30:1 was mixed from 1.33 g (13.5 mmol, 100 eq) **EtOx**, 1.41 g (6.7 mmol, 50 eq) **Dc$^{=}$Ox**, 0.792 g (4 mmol, 30 eq) **TMBO** and 0.025 g (0.13 mmol, 1 eq) **MeOTs**. The mixtures were placed in microwave vials under argon flow, which were sealed with a septum. Microwave irradiation was applied for 1 h at 140 °C. The yellowish products

were subjected to several swelling-recovery-drying cycles in dichloromethane for purification. The yields of the purified gels upon a weight constant were equal to or higher than 95%.

Swelling Degrees. Samples of 0.3 g of each of the purified and carefully dried hydrogels were swollen in excess amounts of deionized water, ethanol or dichloromethane, respectively. The swelling degrees were determined gravimetrically after 24 h in duplicate (referred to as SD1 and SD2), preceded by the removal of excess solvent. The swelling degrees were calculated as the relative differences of masses according to $(m_{swollen} - m_{dry})/m_{dry}$ (Tables 1–5 and Figure 1).

Table 1. The swelling degrees of p**EtOx**$_{150}$-p**TMBO**$_x$ networks in water, ethanol, and dichloromethane. The swelling degrees according to $(m_{swollen} - m_{dry})/m_{dry}$ were determined in duplicate [SD1 and SD2, respectively; the average is represented by the arithmetic mean value (MV) and the standard deviation, σ].

x ↓	H_2O			EtOH			Dichloromethane		
	SD1	SD2	MV ± σ	SD1	SD2	MV ± σ	SD1	SD2	MV ± σ
6	6.6	8.0	7.3 ± 1.0	5.9	5.7	5.8 ± 0.1	7.7	7.8	7.8 ± 0.1
7.5	6.0	6.3	6.2 ± 0.2	5.0	5.2	5.1 ± 0.1	8.4	3.9	6.1 ± 3.2
10	5.1	3.8	4.4 ± 0.1	3.0	3.8	3.4 ± 0.6	5.4	5.2	5.3 ± 0.1
15	2.4	2.8	2.6 ± 0.1	2.3	2.4	2.3 ± 0.1	3.3	3.4	3.3 ± 0.1
30	1.6	1.9	1.8 ± 0.1	1.5	1.8	1.6 ± 0.2	2.7	2.5	2.6 ± 0.1

Table 2. The swelling degrees of p**EtOx**$_{100}$-p**Dc$^{=}$Ox**$_{50}$-p**TMBO**$_x$ networks in water, ethanol and dichloromethane. The swelling degrees according to $(m_{swollen} - m_{dry})/m_{dry}$ were determined in duplicate [SD1 and SD2, respectively; the average is represented by the arithmetic mean value (MV) and the standard deviation, σ].

x ↓	H_2O			EtOH			Dichloromethane		
	SD1	SD2	MV ± σ	SD1	SD2	MV ± σ	SD1	SD2	MV ± σ
6	0.8	0.8	0.8 ± 0.0	5.8	5.6	5.7 ± 0.1	14.2	11.3	12.7 ± 2.0
7.5	0.8	0.7	0.8 ± 0.1	4.4	4.6	4.5 ± 0.1	9.7	8.0	8.9 ± 1.2
10	0.6	0.7	0.7 ± 0.9	4.4	4.0	4.2 ± 0.3	7.5	6.3	6.9 ± 0.9
15	0.8	1.0	0.9 ± 0.5	3.3	3.6	3.4 ± 0.2	5.0	5.7	5.3 ± 0.5
30	0.8	1.0	0.9 ± 0.0	2.1	2.3	2.2 ± 0.2	3.4	3.4	3.4 ± 0.0

Table 3. The swelling degrees of p**EtOx**$_{50}$-p**NonOx**$_{50}$-p**Dc$^{=}$Ox**$_{50}$-p**TMBO**$_x$ networks in water, ethanol and dichloromethane. The swelling degrees according to $(m_{swollen} - m_{dry})/m_{dry}$ were determined in duplicate [SD1 and SD2, respectively; the average is represented by the arithmetic mean value (MV) and the standard deviation, σ].

x ↓	H_2O			EtOH			Dichloromethane		
	SD1	SD2	MV ± σ	SD1	SD2	MV ± σ	SD1	SD2	MV ± σ
6	0.8	1.5	1.2 ± 0.5	5.4	5.1	5.3 ± 0.2	13.3	11.9	12.6 ± 1.0
7.5	0.6	0.6	0.6 ± 0.0	4.1	3.8	3.9 ± 0.2	10.8	10.3	10.5 ± 0.3
10	0.9	1.5	1.2 ± 0.7	3.4	3.2	3.3 ± 0.1	9.1	8.1	8.6 ± 0.7
15	1.2	1.9	1.5 ± 0.6	3.2	4.0	3.6 ± 0.6	7.1	8.0	7.5 ± 0.6
30	1.0	0.7	0.9 ± 0.0	1.9	1.9	1.9 ± 0.0	4.0	4.0	4.0 ± 0.0

Table 4. The swelling degrees of p**NonOx**$_{100}$-p**Dc**$^{=}$**Ox**$_{50}$-p**TMBO**$_x$ networks in water, ethanol and dichloromethane. The swelling degrees according to $(m_{swollen} - m_{dry})/m_{dry}$ were determined in duplicate [SD1 and SD2, respectively; the average is represented by the arithmetic mean value (MV) and the standard deviation, σ].

x ↓	H_2O			EtOH			Dichloromethane		
	SD1	SD2	MV ± σ	SD1	SD2	MV ± σ	SD1	SD2	MV ± σ
6	0.5	0.9	0.7 ± 0.3	1.0	1.2	1.1 ± 0.2	16.6	20.2	18.4 ± 2.5
7.5	0.9	0.7	0.8 ± 0.1	0.7	1.0	0.9 ± 0.2	15.4	18.7	17.1 ± 2.4
10	1.2	0.8	1.0 ± 0.3	1.1	1.1	1.1 ± 0.0	15.3	9.3	12.3 ± 4.2
15	0.5	0.5	0.5 ± 0.2	1.6	1.8	1.7 ± 0.2	8.7	8.9	8.8 ± 0.2
30	1.3	1.6	1.5 ± 0.2	1.7	1.9	1.8 ± 0.2	5.2	5.4	5.3 ± 0.2

Table 5. The swelling degrees of p**NonOx**$_{150}$-p**TMBO**$_x$ networks in water, ethanol and dichloromethane. The swelling degrees according to $(m_{swollen} - m_{dry})/m_{dry}$ were determined in duplicate [SD1 and SD2, respectively; the average is represented by the arithmetic mean value (MV) and the standard deviation, σ].

x ↓	H_2O			EtOH			Dichloromethane		
	SD1	SD2	MV ± σ	SD1	SD2	MV ± σ	SD1	SD2	MV ± σ
7.5	1.0	1.8	1.4 ± 0.5	1.0	1.4	1.2 ± 0.3	23.9	24.2	24.0 ± 0.2
10	0.7	0.6	0.6 ± 2.2	0.9	1.3	1.1 ± 0.3	15.6	18.7	17.1 ± 2.2
15	1.4	0.5	1.0 ± 0.5	1.3	2.3	1.8 ± 0.7	11.4	12.1	11.7 ± 0.5
30	0.7	0.6	0.7 ± 0.1	1.8	2.3	2.0 ± 0.3	5.6	5.4	5.5 ± 0.1

Dye Inclusion. (i) In Situ *Inclusion*: **FITC** was added in 0.2 wt% amounts to the corresponding reaction mixture, yielding 2 g of hydrogel of the composition p**EtOx**$_{100}$-p**Dc**$^{=}$**Ox**$_{50}$-p**TMBO**$_{30}$-**FITC**$_{0.1}$; (ii) *Post-Synthetic Strategy*: Hydrogels of the composition p**EtOx**$_{100}$-p**Dc**$^{=}$**Ox**$_{50}$-p**TMBO**$_6$ (0.5 g) were swollen in a suspension of 50 mg **FITC** in dichloromethane/ethanol (1.5:0.5 mL) for 24 h. After recovery from the clear solutions, the hydrogels were dried and washed multiple times with water. According to gravimetric analysis, the dye was absorbed completely, yielding a hydrogel of the composition p**EtOx**$_{100}$-p**Dc**$^{=}$**Ox**$_{50}$-p**TMBO**$_6$ (**FITC**)$_{2.8}$.

Milling Experiments. Milling experiments were conducted using a Retsch S1000 planetary ball mill. Poly(2-oxazoline)s composed of p**EtOx**$_{100}$-p**DC**$^{=}$**Ox**$_{50}$-p**TMBO**$_6$ (**FITC**)$_{2.8}$ and p**EtOx**$_{100}$-p**Dc**$^{=}$**Ox**$_{50}$-p**TMBO**$_{30}$-**FITC**$_{0.1}$ were ground in aqueous suspensions (100 mg/15 mL) and, in order to prevent reaggregation and to maintain particle sizes in the micrometer-range, were ultrasonicated prior to the size distribution measurements and functionalization, respectively. Particle size distributions were determined in aqueous suspension using a CILAS 1180 Particle Size Analyzer (CILAS, Orleans, France).

Thiol-ene Photoreactions. Fifty milligrams of ground hydrogel of the composition p**EtOx**$_{100}$-p**Dc**$^{=}$**Ox**$_{50}$-p**TMBO**$_{30}$-**FITC**$_{0.1}$ were suspended in 7.5 mL of water and mixed with 2.0 mg of c(RGDfC) and 10 µL of photoinitiator Lucirin TPO-L prior to polychromatic irradiation with 4500 mW·cm^{-2} at a distance of 8 cm to the light source (light guide) and irradiated for 45 min. After completion of the illumination, the suspension was decanted from the insoluble photoinitiator residues/decomposition products and used for the cell tests.

Cell Lines. The human pancreatic BON cell line was established from a human pancreatic carcinoid tumor [36]. BON cells were grown in a 1:1 mixture of Dulbecco's Modified Eagle's Medium (DMEM) and Ham's F-12 medium containing 10% (*v*/*v*) fetal calf serum (FCS) (Biochrom Co., Berlin, Germany) and 1% (*v*/*v*) L-glutamine [37]. The EA.hy926 cell line, which served as a model for endothelial cells, was maintained in DMEM (Biochrom AG, Berlin, Germany) with 10% fetal bovine serum, 100 U/mL penicillin and 100 µg/mL streptomycin [38].

Cell Tests. For microscopic evaluation, cells were seeded on glass cover slips (approximately 20.000/cover slip). After 24 h of adherence, cells were incubated with 2 mL of a hydrogel-containing medium (1:100 dilution of hydrogel stock solutions with 6.7 mg hydrogel/mL) for 3 or 24 h, respectively. Subsequently, the cover slips were gently rinsed in phosphate-buffered saline (PBS) in order to remove non-adhered hydrogel particles. Cover slips were mounted on glass slides and evaluated by transmission light and green fluorescence microscopy.

3. Results and Discussion

*3.1. Synthesis of the Poly(2-oxazoline)-Based Networks and Covalent Attachment of **FITC***

Network synthesis was performed from mixtures of the three monofunctional monomers, **EtOx**, **NonOx** and **Dc$^{=}$Ox**, the crosslinker, **TMBO**, and the initiator, **MeOTs**, in dichloromethane solutions. In order to avoid unfavorably high swelling of the gels under physiological conditions, copolymer networks with a high content of hydrophobic monomers and/or high crosslinking degrees were focused on. All syntheses were performed in individually sealed vials at 140 °C in a single-mode microwave reactor for 1 h in order to reach maximum conversion (Scheme 2). A ratio of **MeOTs** and the sum of **EtOx**, **NonOx** and **Dc$^{=}$Ox** of 1:150 was maintained throughout all syntheses. Five different ratios of [**EtOx**]:[**NonOx**]:[**Dc$^{=}$Ox**] = 150:0:0, 100:0:50, 50:50:50, 0:100:50 and 0:150:0 were used for the hydrogel syntheses, concomitant with a variation of the crosslinker, **TMBO**, in the range of 150:30, 150:15, 150:10, 150:7.5 or 150:6 (corresponding to ratios of 5:1, 10:1, 15:1, 20:1 and 25:1) for all series.

Comparably low degrees of crosslinking, such as 150:3 (50:1), yielded crosslinked copoly(2-oxazoline)s, which dissolved in dichloromethane during purification. Hence, this study was limited to networks with the lowest crosslinking degrees of 150:6. Concomitantly, a network library of 5 × 5 = 25 members was obtained from one-pot/one-step strategies analogous to a previously developed recipe [30]. The gels were recovered as pre-swollen networks of a yellowish color, dried under reduced pressure and subjected to repeated swelling-recovery-drying cycles in dichloromethane, until a weight constant of the dried gels was achieved. Yields of the colorless to yellowish purified hydrogels were 95% or higher.

Due to its functional groups, **FITC** can act as a terminating agent in cationic ring-opening polymerizations (Scheme 1): The addition of small amounts of **FITC** to the initial reaction mixture yielded networks with covalently bound **FITC**, which was validated on the example of the network, p**EtOx**$_{100}$-p**Dc$^{=}$Ox**$_{50}$-p**TMBO**$_{30}$-**FITC**$_{0.1}$. Correspondingly functionalized hydrogels could be ground in a ball mill in order to yield microparticles (see the section "Milling Experiments").

3.2. Swelling Degrees and Polymeranalogous Compound Loading

The swelling degrees were determined in water, ethanol and dichloromethane as test solvents after 24 h (Figure 1). Only an insignificant further increase of the swelling degrees was observed after that period; swelling degrees were determined in duplicate. The gels that were composed exclusively of **EtOx** as a monofunctional monomer showed fairly comparable swelling in all three test solvents: in the p**EtOx**$_{150}$-p**TMBO**$_x$ series, swelling degrees only depended on the degree of crosslinking with maximum swelling degrees of eight for crosslinking degrees of 150:6. Due to their comparable swelling degrees in water, ethanol and dichloromethane, these gels may be referred to as amphigels.

Figure 1. Swelling degrees of poly(2-oxazoline)-based gels of the composition (**a**) p**EtOx**$_{150}$-p**TMBO**$_x$; (**b**) p**EtOx**$_{100}$-p**Dc$^{=}$Ox**$_{50}$-p**TMBO**$_x$; (**c**) p**EtOx**$_{50}$-p**NonOx**$_{50}$-p**Dc$^{=}$Ox**$_{50}$-p**TMBO**$_x$; (**d**) p**NonOx**$_{100}$-p**Dc$^{=}$Ox**$_{50}$-p**TMBO**$_x$ and (**e**) p**NonOx**$_{150}$-p**TMBO**$_x$ in water, ethanol and dichloromethane; *x* comprises the value range of 6, 7.5, 10, 15 and 30.

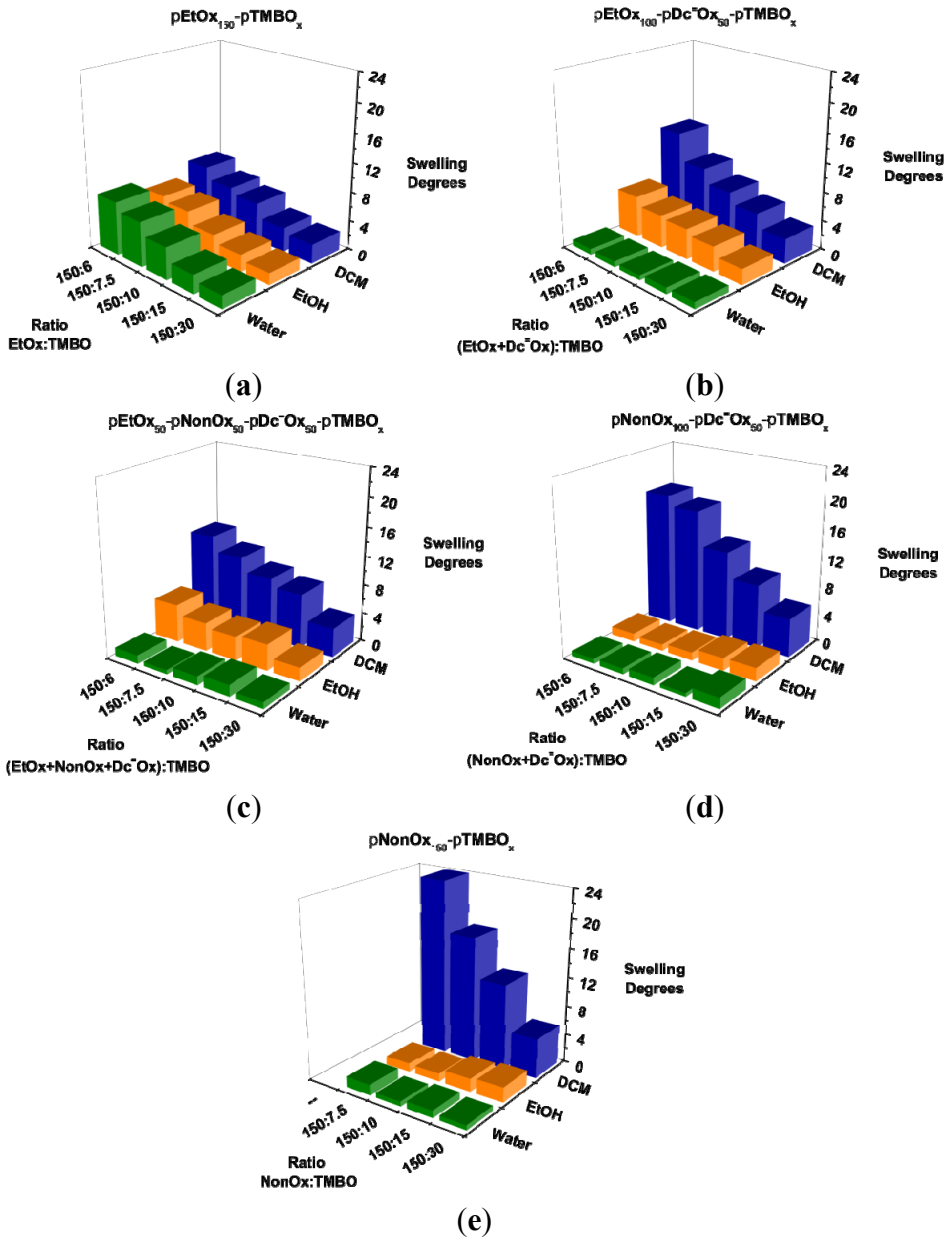

The networks composed of **EtOx** and **Dc$^{=}$Ox**, as well as those composed of **EtOx** and **NonOx**, as well as **Dc$^{=}$Ox** exhibited hardly any swelling in water, reasonable swelling in ethanol and high swelling in dichloromethane: due to the reasonable swelling in ethanol, the networks of the compositions p**EtOx**$_{100}$-p**Dc$^{=}$Ox**$_{50}$-p**TMBO**$_x$ and p**EtOx**$_{50}$-p**NonOx**$_{50}$-p**Dc$^{=}$Ox**$_{50}$-p**TMBO**$_x$ still may be referred to as amphigels. Their swelling degrees were quasi-constant in water (one or lower) and increased with decreasing crosslinking degrees in the other two test solvents to maximum values of approximately five in ethanol and approximately 13 in dichloromethane.

Networks that did not contain any p**EtOx** swelled only in dichloromethane and can most adequately be described as lipogels. Maximum swelling degrees in the series p**NonOx**$_{100}$-p**Dc$^{=}$Ox**$_{50}$-p**TMBO**$_x$ and p**NonOx**$_{150}$-p**TMBO**$_x$ were in the range of 20. Notably, insoluble networks in the p**NonOx**$_{150}$-p**TMBO**$_x$ series were only obtained for crosslinking degrees up to 150:7.5.

In addition to *in situ* functionalization (Section 3.1.), the poly(2-oxazoline)-based gels could also be modified post-synthetically in order to subsequently act as loaded drug carriers: networks with comparably high swelling in dichloromethane and low or no swelling in water, for example, could be impregnated post-synthetically with organic molecules during swelling in dichloromethane (diffusion-mediated inclusion of the organic molecules into the networks). After recovery and drying of the networks, the organic molecules were not released from dried non-degraded hydrogels in aqueous environments. The loading of hydrogels of the composition p**EtOx**$_{100}$-p**Dc$^{=}$Ox**$_{50}$-p**TMBO**$_6$ with **FITC** as the model compound was accomplished from dichloromethane:ethanol = 3:1 *v*/*v* suspensions of the fluorescent dye. Within 24 h, the suspension cleared and no solid residues of **FITC** could be detected. According to gravimetric control, **FITC** was included in the network (quasi-)quantitatively, yielding a gel of the composition p**EtOx**$_{100}$-p**Dc$^{=}$Ox**$_{50}$-p**TMBO**$_6$ (**FITC**)$_{2.8}$. Notably, this strategy paves the way for the loading of the gels with drugs at room temperature, overcoming the risk of the decomposition of the drugs at high temperatures, like those during the polymerization.

3.3. Milling Experiments

Milling experiments were performed with hydrogels of the composition p**EtOx**$_{100}$-p**Dc$^{=}$Ox**$_{50}$-p**TMBO**$_6$ (**FITC**)$_{2.8}$ and p**EtOx**$_{100}$-p**Dc$^{=}$Ox**$_{50}$-p**TMBO**$_{30}$-**FITC**$_{0.1}$. Both networks could not be successfully ground in a ball mill in the dry state, but only as aqueous suspensions (100 mg/15 mL), yielding particles with dimensions in the micrometer range (Figure 2a). The ground particles tended to re-aggregate and, upon water removal under reduced pressure, correspondingly yielded films instead of powders. Even by the application of ultrasound for several hours, these films could not be re-suspended in water to yield microparticles. Hence, the micrometer range of the microparticle size distribution was only stable in aqueous media for a limited time. Even though the tendency of the particles to re-aggregate in aqueous media was lowered, the application of ultrasound was required for the re-establishment of the microparticle size distribution after storage in the range of hours or longer. Currently on-going investigations aim at the addition of (biocompatible) tensides to the mixture during grinding. The first experiments with sodium dodecyl sulfate (SDS), which has been approved as an excipient in mixtures of hydrogel/SDS/water = 100 mg/100 mg/15 mL, have revealed a shift of microparticle size distribution to the lower micrometer range (Figure 2b), while the storage stability,

however, was not in the day range yet, and the suspensions still needed to be ultrasonicated prior to application. Nonetheless, the proof-of-concept that smaller particles need surfactants for stabilization could be established.

Figure 2. Particle size distributions of p**EtOx**$_{100}$-p**Dc**$^{=}$**Ox**$_{50}$-p**TMBO**$_6$ gels that were ground in a ball mill as aqueous suspensions for 24 h: feeds of 100 mg gel in 15 mL of water (**a**: 10%/50% particle size diameter after grinding = 0.80/3.06 µm) and feeds of 100 mg·gel, 100 mg of sodium dodecyl sulfate (SDS) and 15 mL of water (**b**: 10%/50% particle size diameter after grinding = 0.72/2.33 µm).

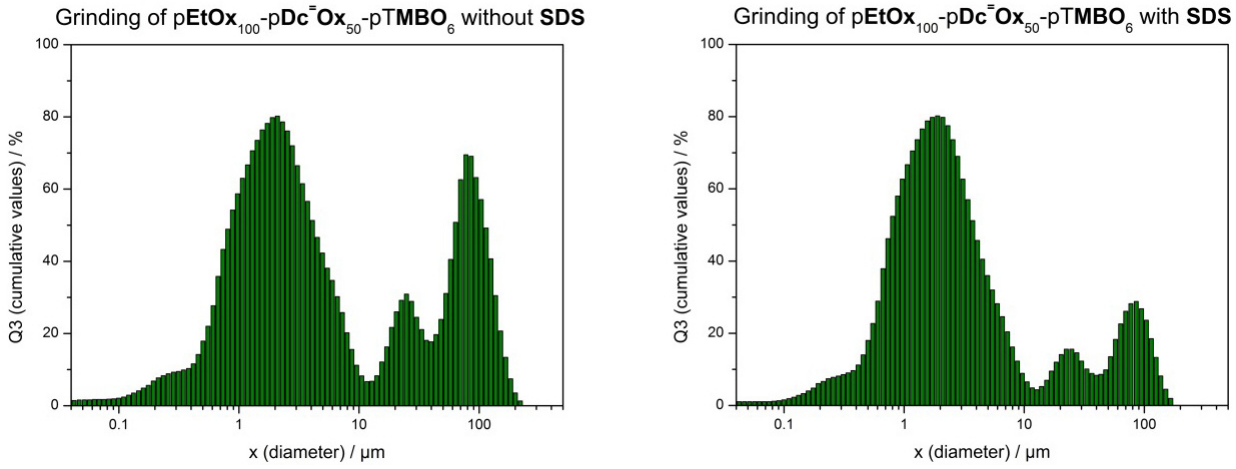

(a) **(b)**

3.4. Surface Functionalization

The UV-induced crosslinking of poly(2-oxazoline)-based copolymers with oligovalent thiols and the functionalization of decenyl side-chains of poly(2-oxazoline)s by thiol-ene reactions have been described in the literature [31–33]. In this study, the concept was transferred to the functionalization of ground gel particles in suspension by thiol-ene reactions, benefiting from the fact that they are insensitive to water [39]. The cyclic pentapeptide, c(RGDfC), was chosen, because of its enhanced cancer cell recognition, due to the RGD motif geometrically constrained in the pentacycles bearing a bulky D-amino acid (D-phenylalanine in this case) [15,18,19] and the presence of the thiol-bearing L-cysteine for thiol-ene reactions. After UV-irradiating a mixture of the peptide and the freshly ground, **FITC**-functionalized hydrogel, the suspension was used for cell tests (see below). In order to prove that the RGD functionalization was successful and that it had occurred preferentially at the microgel surface, a cross-section was cut with a razor blade from particles with diameters in the 150 µm range and subjected to SEM-EDX measurements that revealed the elemental mapping of carbon, oxygen and sulfur throughout the inner and the outer domains (Figure 3). While carbon and oxygen atoms constituting the polymer network were evenly distributed on the surface of the microgel particle, as well as its interior, sulfur atoms were predominantly detected on the surface of the particle. This finding strongly suggests that the sulfur-containing thiol groups are attached to the microgel surface and supports the claim of the surface functionalization with the RGD motif.

Figure 3. Scanning electron microscopy image of the cross-section of a poly(2-oxazoline)-based gel after grinding and subsequent surface functionalization by (**a**) UV-induced thiol-ene reactions; (**b**) as well as the SEM-EDX images of the cross-section showing the distribution of carbon atoms; (**c**) oxygen atoms; and (**d**) sulfur atoms, respectively. The center plain visible in the images was the interior of the particle prior to cross-sectioning, while all other plains and edges represent the surface.

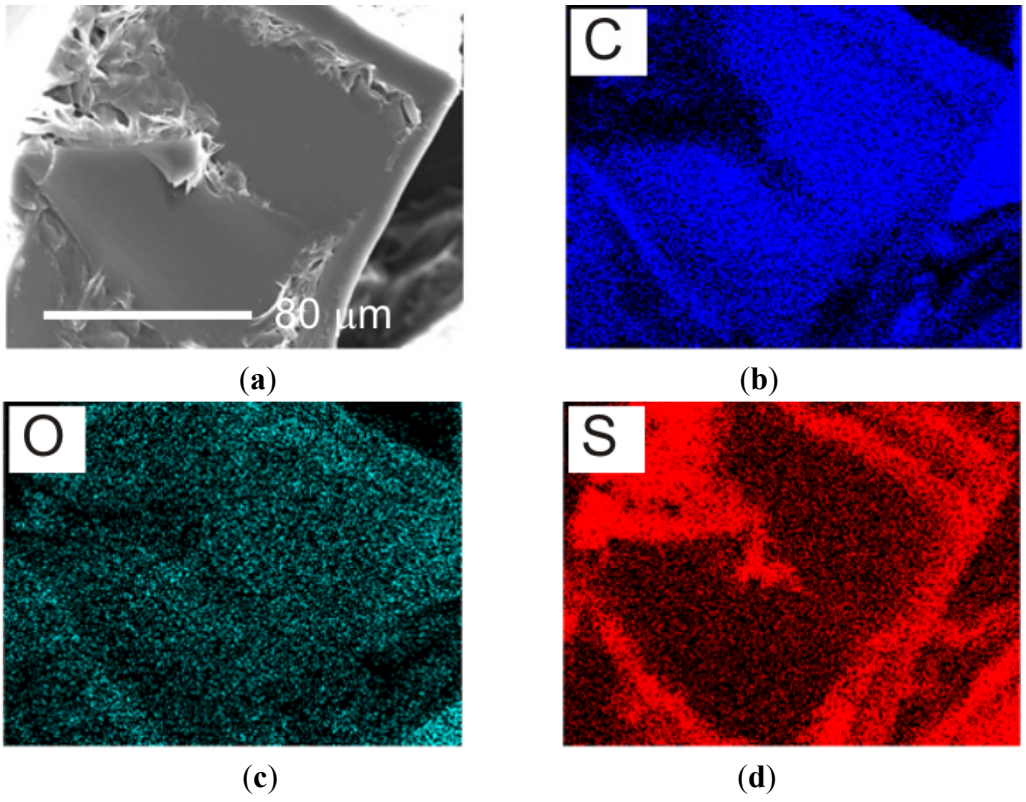

3.5. Cell Tests

The adhesion of freshly ultrasonicated suspensions of ground microgels (p**EtOx**$_{100}$-p**Dc**$^{=}$**Ox**$_{50}$-p**TMBO**$_{30}$-**FITC**$_{0.1}$) with or without RGD-surface functionalization were tested against endothelial EA.hy cells and human pancreatic cancer BON cells [38–41]. BON cells were chosen, because of their pronounced surface expression of highly active $\alpha_v\beta_5$-integrins, according to fluorescence-activated cell sorting measurements [42]. The $\alpha_v\beta_5$-integrin, like its $\alpha_v\beta_3$ congener, has been reported to show an interaction of supreme strength with the RGD motif in peptide pentacycles [18,19]. In order to investigate the adherence of microparticles to these types of cells, the cells were seeded on glass cover slips and incubated with the hydrogel-containing media. Subsequently, the cover slips were gently rinsed in PBS to remove non-adhered hydrogel particles. Samples were then evaluated by transmission light and green fluorescence microscopy.

Due to the covalent attachment of **FITC**, fluorescence microscopy enabled the clear recognition of the microgel particles (Figure 4). In all experiments, only adhesion, but no cellular uptake, of the hydrogels was observed. In n = 5 independent experiments, the time-dependent adherence of RGD-functionalized *vs*. RGD-free hydrogels to BON cells after 24 h was analyzed for $n \geq 350$ cells/type of hydrogel, revealing an approximately 4.3-fold higher adhesion of RGD-bearing hydrogels compared

to the RGD-free ones. Only in RGD-functionalized hydrogels were multiple attachments of several hydrogel-particles to BON cells observed, while RDG-free hydrogels showed only single and random attachments to individual BON cells.

Figure 4. Superimposed transmission and fluorescence photographs of EA.hy endothelial (top) and BON cancer cells (bottom) that were incubated with p**EtOx**$_{100}$-p**Dc**$^{=}$**Ox**$_{50}$-p**TMBO**$_{30}$-**FITC**$_{0.1}$ hydrogels for 3 h (left) and 24 h (right), respectively. Significant adhesion of the hydrogels to cells was only observed for the combination RGD-functionalized particles/BON cancer cells.

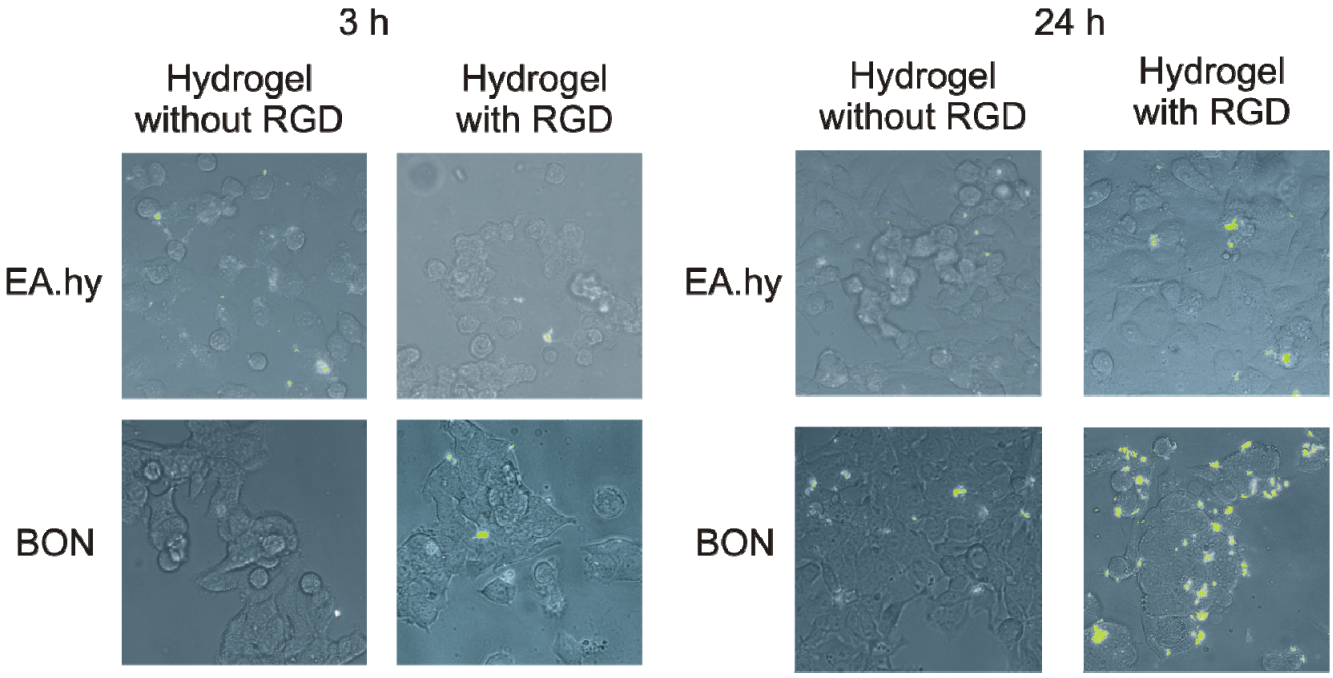

Additionally, control experiments were performed with non-transformed low $\alpha_v\beta_5$-expressing endothelial EA.hy cells: significant adhesion of the particles to the cells could not be observed, neither as a function of time nor as a function of the RGD-functionalization (Figure 4, top). These observations supported the enhanced attachment of RGD-functionalized gels to $\alpha_v\beta_5$-expressing tumor cells. The adhesion of larger particles to the cells is likely to be caused by mechanical interlocking and is not indicative of adhesion due to specific microgel-cell interactions.

4. Conclusions and Outlook

Aiming at the development of novel drug delivery systems for chemotherapeutics, poly(2-oxazoline)-based hydrogels were surface-functionalized with a pentacyclic RGD motif for integrin recognition at cancer cell surfaces. The swelling degrees in water, ethanol and dichloromethane of the copoly(2-oxazoline)-based networks composed of aliphatic 2-oxazolines can be adjusted by the variation of the monomers, namely **EtOx**, **NonOx** and **Dc**$^{=}$**Ox**. This allows for one-pot/one-step syntheses of amphi- and lipo-gels that could be loaded with compounds *in situ* or post-synthetically. The incorporation of **Dc**$^{=}$**Ox** into the networks enabled the surface functionalization of (ground) gels by photo-initiated thiol-ene reactions with the cyclic peptide, c(RGDfC).

Microparticles bearing covalently surface-bound RGD peptide sequences were found to adhere to BON cancer cells to significant degrees, while hardly any adherence to non-cancerous human endothelial cells could be observed. This preferential adhesion makes these microgels potential candidates for the delivery of otherwise non-selective chemotherapeutics to cancer cells. Notably, multiple adhesions to adjacent cancer cells could be observed for RGD-functionalized particles.

Current investigations aim at optimizing the grinding procedure, in particular, by stabilizing the particle size distribution in a suspension (additives for the stabilization of the particle size distribution), and the introduction of stimuli-responsive chemical linkers for the attachment of chemotherapeutics. While poly(2-oxazoline)s are stable towards hydrolysis under physiological conditions [43], acid-labile linkers are one key strategy for the introduction of stimuli-responsive bonds. Hence, drug release will be triggered only at the targeted cells.

Acknowledgments

This study was performed at Polymer Competence Center Leoben GmbH (PCCL), the Institute for Chemistry and Technology of Materials of the Graz University of Technology and the Department of Physiology of Charité Berlin. PCCL is funded by the Austrian Government and the State Governments of Styria and Upper Austria within the framework of the Kplus-program of the Austrian Ministry of Traffic, Innovation and Technology. Michael Höpfner was supported by the Schüchtermann-Stiftung, Germany.

Conflicts of Interest

The authors declare no conflict of interest.

References

1. Qiu, Y.; Park, K. Environment-sensitive hydrogels for drug delivery. *Adv. Drug Deliv. Rev.* **2001**, *53*, 321–339.
2. Knop, K; Hoogenboom, R.; Fischer, D.; Schubert, U.S. Poly(ethylene glycol) in drug delivery: Pros and cons as well as potential alternatives. *Angew. Chem. Int. Ed.* **2010**, *49*, 6288–6308.
3. Puskas, J.E.; Chen, Y. Biomedical application of commercial polymers and novel polyisobutylene-based thermoplastic elastomers for soft tissue replacement. *Biomacromolecules* **2004**, *5*, 1141–1154.
4. Lee, K.Y.; Mooney, D.J. Hydrogels for tissue engineering. *Chem. Rev.* **2001**, *101*, 1869–1880.
5. Bae, Y.; Fukushima, S.; Harada, A.; Kataoka, K. Design of environment-sensitive supramolecular assemblies for intracellular drug delivery: Polymeric micelles that are responsive to intracellular pH change. *Angew. Chem. Int. Ed.* **2003**, *42*, 4640–4643.
6. Ulbrich, K.; Subr, V.; Podperova, P.; Buresova, M. Synthesis of novel hydrolytically degradable hydrogels for controlled drug release. *J. Control. Release* **1995**, *34*, 155–165.
7. Kelly, A.M.; Wiesbrock, F. Strategies for the synthesis of poly(2-oxazoline)-based hydrogels. *Macromol. Rapid Commun.* **2012**, *33*, 1632–1647.
8. Hoogenboom, R.; Schlaad, H. Bioinspired poly(2-oxazoline)s. *Polymers* **2011**, *3*, 467–488.

9. Farrugia, B.L.; Kempe, K.; Schubert, U.S.; Hoogenboom, R.; Dargaville, T.R. Poly(2-oxazoline) hydrogels for controlled fibroblast attachment. *Biomacromolecules* **2013**, *14*, 2724–2732.
10. Deng, X.; Eyster, T.W.; Elkasabi, Y.; Lahann, J. Bio-orthogonal polymer coatings for co-presentation of biomolecules. *Macromol. Rapid Commun.* **2012**, *33*, 640–645.
11. Paterson, S.M.; Shadforth, A.M.A.; Shaw, J.A.; Brown, D.H.; Chirila, T.V.; Baker, M.V. Improving the cellular invasion into PHEMA sponges by incorporation of the RGD peptide ligand: The use of copolymerization as a means to functionalize PHEMA. *Mater. Sci. Eng. C Biol. Sci.* **2013**, *33*, 4917–4922.
12. Jabbari, E.; He, X.; Valarmathi, M.T.; Sarvestani, A.S.; Xu, W.J. Material properties and bone marrow stromal cells response to *in situ* crosslinkable RGD-functionalized lactide-*co*-glycolide scaffolds. *Biomed. Mater. Res. A* **2009**, *89A*, 124–137.
13. Hansson, A.; Hashom, N.; Falson, F.; Rousselle, P.; Jordan, O.; Borchard, G. *In vitro* evaluation of an RGD-functionalized chitosan derivative for enhanced cell adhesion. *Carbohydr. Polym.* **2012**, *90*, 1494–1500.
14. Liu, X.; Peng, W.; Wang, Y.; Zhu, M.; Sun, T.; Peng, Q.; Zeng, Y.; Feng, B.; Lu, X.; Weng, J.; *et al*. Synthesis of an RGD-grafted oxidized sodium alginate-N-succinyl chitosan hydrogel and an *in vitro* study of endothelial and osteogenic differentiation. *J. Mater. Chem. B* **2013**, *1*, 4484–4492.
15. Haubner, R.; Schmitt, W.; Hölzemann, G.; Goodman, S.L.; Jonczyk, A.; Kessler, H. Cyclic RGD peptides containing β-turn mimetics. *J. Am. Chem. Soc.* **1996**, *118*, 7881–7891.
16. Kessler, H. Conformation and biological activity of cyclic peptides. *Angew. Chem. Int. Ed.* **1982**, *21*, 512–523.
17. Zhu, S.; Zhang, J.; Janjana, J.; Vegesna, G.; Tiwari, A.; Luo, F.-T.; Wei, J.; Liu, H. Highly water-soluble, near-infrared emissive BODIPY polymeric dye bearing RGD peptide residues for cancer imaging. *Anal. Chim. Acta* **2013**, *758*, 138–144.
18. Meyer, A.; Auernheimer, J.; Modlinger, A.; Kessler, H. Targeting RGD recognizing integrins: Drug development, biomaterial research, tumor imaging and targeting. *Curr. Pharm. Des.* **2006**, *12*, 2723–2747.
19. Wang, F.; Li, Y.; Shen, Y.; Wang, A.; Wang, S.; Xie, T. The functions and applications of RGD in tumor therapy and tissue engineering. *Int. J. Mol. Sci.* **2013**, *14*, 13447–13462.
20. Danhier, F.; le Breton, A.; Preat, V. RGD-based strategies to target alpha(v) beta(3) integrin in cancer therapy and diagnosis. *Mol. Pharm.* **2012**, *9*, 2961–2973.
21. Hynes, R.O. A reevaluation of integrins as regulators of angiogenesis. *Nat. Med.* **2002**, *8*, 918–921.
22. Aydin, D.; Louban, I.; Perschmann, N.; Blümmel, J.; Lohmüller, T.; Cavalcanti-Adam, E.A.; Haas, T.L.; Walczak, H.; Kessler, H.; Fiammengo, R.; *et al*. Polymeric substrates with tunable elasticity and nanoscopically controlled biomolecule presentation. *Langmuir* **2010**, *26*, 15472–15480.
23. Hoogenboom, R. Poly(2-oxazoline)s: A polymer class with numerous potential applications. *Angew. Chem. Int. Ed.* **2009**, *48*, 7978–7994.
24. Wiesbrock, F.; Hoogenboom, R.; Schubert, U.S. Microwave-assisted polymer synthesis: State-of-the-art and future perspectives. *Macromol. Rapid Commun.* **2004**, *25*, 1739–1764.

25. Wiesbrock, F.; Hoogenboom, R.; Leenen, M.A.M.; Meier, M.A.R.; Schubert, U.S. Investigation of the living cationic ring-opening polymerization of 2-methyl-, 2-ethyl-, 2-nonyl-, and 2-phenyl-2-oxazoline in a single-mode microwave reactor. *Macromolecules* **2005**, *38*, 5025–5034.
26. Wiesbrock, F.; Hoogenboom, R.; Leenen, M.A.M.; van Nispen, S.F.G.M.; van der Loop, M.; Abeln, C.H.; van den Berg, A.M.; Schubert, U.S. Microwave-assisted synthesis of a 4^2-membered library of diblock copoly(2-oxazoline)s and chain-extended homo poly(2-oxazoline)s and their thermal characterization. *Macromolecules* **2005**, *38*, 7957–7966.
27. Ebner, C.; Bodner, T.; Stelzer, F.; Wiesbrock, F. One decade of microwave-assisted polymerizations: Quo vadis? *Macromol. Rapid Commun.* **2011**, *32*, 254–288.
28. Bodner, C.; Ellmaier, L.; Schenk, V.; Albering, J.; Wiesbrock, F. Delocalized π-electrons in 2-oxazoline rings in negatively charged nitrogen atoms: Revealing the selectivity during the initiation of cationic ring-opening polymerizations. *Polym. Int.* **2011**, *60*, 1173–1179.
29. Rossegger, E.; Schenk, V.; Wiesbrock, F. Design strategies for functionalized poly(2-oxazoline)s and derived materials. *Polymers* **2013**, *5*, 956–1011.
30. Kelly, A.M.; Hecke, A.; Wirnsberger, B.; Wiesbrock, F. Synthesis of poly(2-oxazoline)-based hydrogels with tailor-made swelling degrees capable of stimuli-triggered compound release. *Macromol. Rapid Commun.* **2011**, *32*, 1815–1819.
31. Schenk, V.; Ellmaier, L.; Rossegger, E.; Edler, M.; Griesser, T.; Weidinger, G.; Wiesbrock, F. Water-developable poly(2-oxazoline)-based negative photoresist. *Macromol. Rapid Commun.* **2012**, *33*, 396–400.
32. Kempe, K.; Hoogenboom, R.; Schubert, U.S. A green approach for the synthesis and thiol-ene modification of alkene functionalized poly(2-oxazoline)s. *Macromol. Rapid Commun.* **2011**, *32*, 1484–1489.
33. Diehl, C.; Schlaad, H. Polyoxazoline-based crystalline microspheres for carbohydrate-protein recognition. *Chem. Eur. J.* **2009**, *15*, 11469–11472.
34. Witte, H; Seeliger, W. Cyclische imidsäureester aus nitrilen und aminoalkoholen. *Liebigs Ann. Chem.* **1974**, *1974*, 996–1009.
35. Beck, M.; Birnbrich, P.; Eicken, U.; Fischer, H.; Fristad, W.E.; Hase, B.; Krause, H.-J. Polyoxazoline auf fettchemischer Basis. *Angew. Makromol. Chem.* **1994**, *223*, 217–233.
36. Evers, B.M.; Townsend Jr., C.M.; Upp, J.R.; Allen, E.; Hurlbut, S.C.; Kim, S.W.; Rajaraman, S.; Singh, P.; Reubi, J.C.; Thompson J.C. Establishment and characterization of a human carcinoid in nude mice and effect of various agents on tumor growth. *Gastroenterology* **1991**, *101*, 303–311.
37. Gloesenkamp, C.; Nitzsche, B.; Lim, A.R. Normant, E.; Vosburgh, E.; Schrader, M.; Ocker, M.; Scherübl, H.; Höpfner, M. AKT inhibition by triciribine alone or as combination therapy for growth control of gastroenteropancreatic neuroendocrine tumors. *Int. J. Oncol.* **2012**, *40*, 876–888.
38. Edgell, C.-J.S.; McDonald, C.C.; Graham, J.B. Permanent cell line expressing human factor VIII-related antigen established by hybridization. *Proc. Natl. Acad. Sci. USA* **1983**, *80*, 3734–3737.
39. Kade, M.J.; Burke, D.J.; Hawker, C.J. The power of thiol-ene chemistry. *J. Polym. Sci. Part A Polym. Chem.* **2010**, *48*, 743–750.

40. Höpfner, M.; Baradari, V.; Huether, A.; Schöfl, C.; Scherübl, H. The insulin-like growth factor receptor 1 is a promising target for novel treatment approaches in neuroendocrine gastrointestinal tumors. *Endocr. Relat. Cancer* **2006**, *13*, 135–149.
41. Höpfner, M.; Schuppan, D.; Scherübl, H. Treatment of gastrointestinal neuroendocrine tumors with inhibitors of growth factor receptors and their signaling pathways: Recent advances and future perspectives. *World J. Gastroenterol.* **2008**, *14*, 2461–2473.
42. Fechner, H.; Wang, X.; Wang, H.; Jansen, A.; Pauschinger, M.; Scherübl, H.; Bergelson, J.M.; Schultheiss, H.-P.; Poller, W. Trans-complementation of vector replication *vs*. coxsackie-adenovirus-receptor overexpression to improve transgene expression in poorly permissive cancer cells. *Gene Ther.* **2000**, *7*, 1954–1968.
43. Kelly, A.M.; Kaltenhauser, V.; Mühlbacher, I.; Rametsteiner, K.; Kren, H.; Slugovc, C.; Stelzer, F.; Wiesbrock, F. Poly(2-oxazoline)-derived contact biocides: Contributions to the understanding of antimicrobial activity. *Macromol. Biosci.* **2013**, *13*, 116–125.